

High-Power MUTC Photodetectors for RF Photonic Links

Steven Estrella*^a, Leif A. Johansson^a, Milan L. Mashanovitch^a, Andreas Beling^b

^aFreedom Photonics LLC, 41 Aero Camino, Santa Barbara, CA, USA 93117;

^bUniversity of Virginia, 351 McCormick Rd., Charlottesville, VA USA 22904

ABSTRACT

High power photodiodes are needed for a range of applications. The high available power conversion efficiency makes these ideal for antenna remoting applications, including high power, low duty-cycle RF pulse generation. The compact footprint and fiber optic input allow densely packed RF aperture arrays with low cross-talk for phased high directionality emitters. Other applications include linear RF photonic links and other high dynamic range optical systems. Freedom Photonics has developed packaged modified uni-traveling carrier (MUTC) photodetectors for high-power applications. Both single and balanced photodetector pairs are mounted on a ceramic carrier, and packaged in a compact module optimized for high power operation. Representative results include greater than 100 mA photocurrent, >100m W generated RF power and >20 GHz bandwidth. In this paper, we evaluate the saturation and bandwidth of these single ended and balanced photodetectors for detector diameter in the 16 μm to 34 μm range. Packaged performance is compared to chip performance. Further new development towards the realization of >100GHz packaged photodetector modules with optimized high power performance is described. Finally, incorporation of these photodetector structures in novel photonic integrated circuits (PICs) for high optical power application areas is outlined.

Keywords: High-power photodetectors, RF photonics, MUTC, Analog communications, RF over fiber, Linear photodetectors

1. INTRODUCTION

RF photonic links have recently seen an increase in both interest and application, such as antenna remoting, beam forming, optical communications¹, and photonic signal processing². The use of a high-power, high-linearity and wideband photodetector, can vastly improve the system performance with an increase in both spurious-free dynamic range (SFDR) and noise figure (NF)^{3,4}. A uni-traveling carrier (UTC) photodetector with such qualities was first developed by Ishibashi *et al*⁵ and has seen significant development over the years⁶. Recent development has resulted in a modified UTC (MUTC) surface illuminated photodetector with enhancements in both saturation output power and bandwidth⁷, with demonstrated output power up to 32.7 dBm at 15 GHz⁸, and 9.6 dBm at 100 GHz⁹.

Freedom Photonics has developed and packaged the MUTC photodiode technology into a compact footprint photodetector module for that exhibits greater than 100 mA photocurrent, >100 mW output RF power, and a bandwidth >20 GHz¹⁰. Photodetectors with this level of performance could be used in a variety of applications, especially where high linearity / high dynamic range are critical, such as optically remote sensor systems¹¹. In phased-array antenna (PAA) systems, the element spacing limits the operating frequency range, while the number of elements determines the resolution. Our packaged photodetector footprint allows for $\lambda/2$ element spacing in the X-band, while the same device technology could be utilized in a photonic integrated circuit for PAAs operating at >100 GHz. Low-duty cycle high peak power RF pulse generation has been demonstrated with the MUTC photodiode¹², and is particularly attractive for arbitrary waveform generation (AWG), pulsed radar systems, and ultra-wideband (UWB) based wireless communications¹³. While single photodetectors offer numerous advantages, balanced photodetectors are required for noise reduction of common signals, such as laser relative intensity noise (RIN), in order to increase SFDR in analog photonic links. Recent progress in the development of packaged high-power MUTC photodetectors will be presented. Consideration will be given first to device design and fabrication. Next, characterization results will be shown for both single and balanced devices. Lastly, applications will be presented whereby photonic integration of the technology is needed to address high performance systems.

*steven@freedomphotonics.com; phone 1 805 967-4900; fax 1 815 550-1694; freedomphotonics.com

2. DESIGN AND FABRICATION

2.1 MUTC Photodetector Device Design

The UTC photodiode (PD) offers superior performance over a p-i-n photodiode, both in bandwidth and output power. In a UTC design, only the photo-generated minority carriers (electrons) in the undepleted p-type InGaAs absorption layer contribute to the charge transport. Since only fast electrons are injected into the transparent, depleted drift layer, the carrier transit time is generally shorter than for a p-i-n photodiode, which suffers from the slower hole velocity. Recently, the UTC structure has been modified to improve high-power capability and responsivity while maintaining high bandwidth⁷. By inserting an undoped InGaAs layer with an appropriate thickness between the undepleted InGaAs absorption layer and the InP drift layer, the responsivity of the UTC photodiode can be increased. The InP drift layer is n-doped to act as a charge-compensation layer to reduce the space-charge screening effect at high current density. A charge compensation layer predistorts the built-in electric field in order to achieve a flat electric field profile at high current densities. In addition, a cliff layer is used to enhance the electric field in the depleted portion of the absorption layer in order to assist electron transport at the heterojunction interface at high photocurrent. The built-in electric field in the graded doped absorption layer assists diffusion of the photogenerated electrons, which further enhances the bandwidth. The MUTC PD with charge-compensation and cliff layer has mitigated the space-charge effect to the extent that thermal failure has become a primary limiting factor at high power levels. To improve thermal dissipation back-illuminated MUTC photodiode chips were flip-chip bonded to a ceramic submount with high thermal conductivity. The photodetector epitaxial stackup and a flip-chip bonded device are shown in Figure 1.

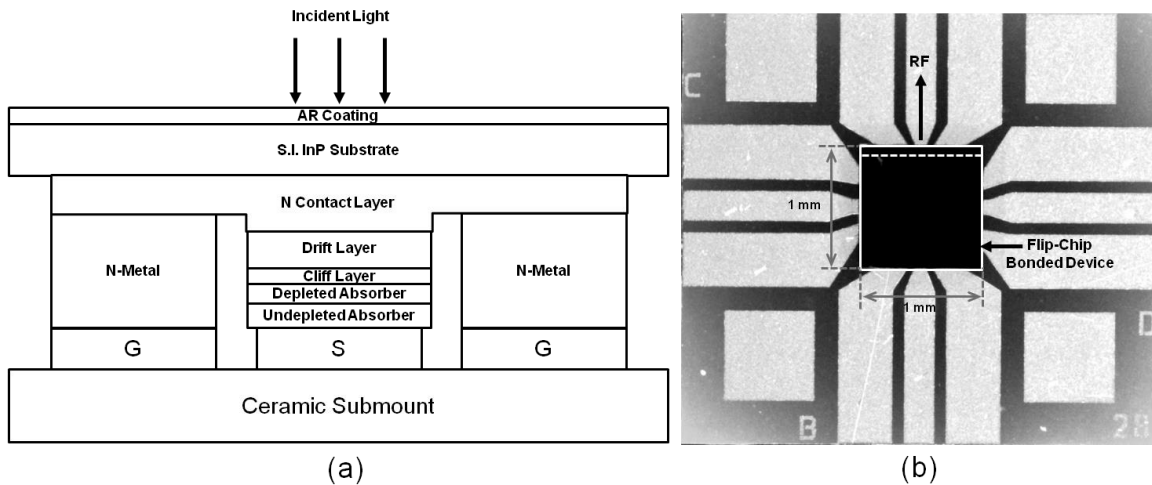


Figure 1. (a) Cross-section description of back-illuminated MUTC photodiode, including coplanar waveguide (CPW) transmission line (ground-signal-ground, GSG) on ceramic submount and epitaxial layer stack-up. (b) Microscope image of MUTC photodetector device flip-chip bonded to ceramic submount, with a white dashed line to give cross-section reference, and solid white line to indicate footprint.

Freedom Photonics' MUTC photodiodes were fabricated on a 3" diameter semi-insulating InP substrate, utilizing our advanced fabrication process portfolio, and following the fabrication process reported for the MUTC⁷. Photodiode active regions were designed using four different diameters, spanning from 16 μm to 34 μm , in order to quantify the tradeoff in maximum RF output and RF bandwidth. The p- and n-mesa structures of the photodiode were patterned using an inductively coupled plasma (ICP) dry etch. The p- and n-contacts to the photodiode were made using an ICP etch and electron-beam metal deposition process. A low-stress dielectric was used for passivation of the mesa structure, in order to reduce leakage current due to defects and surface recombination.

In Figure 2, dark current summary statistics are given from wafer level measurements, for photodiode active region diameters of 16, 20, 28, and 34 μm . From the data, a mean dark current of 79.1 nA, 164.4 nA, 429.8 nA, and 458.4 nA were measured a bias voltage of -5V, for diameters of 16, 20, 28, and 34 μm , respectively. The moderately high leakage current values are primarily attributed to the quality of the dielectric film used for passivation. As expected, the leakage current increases for increasing active region diameter.

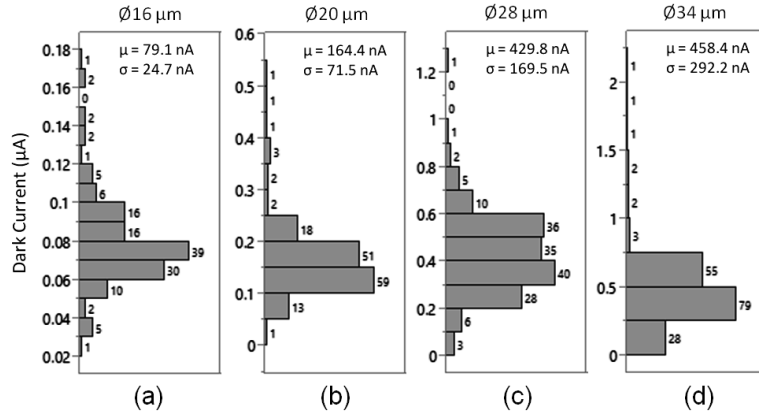


Figure 2. Dark current μ distributions of fabricated single and balanced photodiodes, for active region diameters of (a) 16 μm with mean dark current $\mu = 79$ nA, (b) 20 μm with mean dark current $\mu = 164$ nA, (c) 28 μm with mean dark current $\mu = 430$ nA, and (d) 34 μm with mean dark current $\mu = 458$ nA.

3. RESULTS AND DISCUSSION

3.1 Single Photodetectors

To quantify the performance of the photodetectors, a test setup was constructed as shown in Figure 3. A continuous-wave (CW) laser source is sent through a polarization controller (Pol), before entering a high-speed Mach-Zehnder modulator (MZM). A CW RF tone is generated by the vector network analyzer (VNA), and amplified by a wideband RF amplifier before entering the MZM. The DC bias was provided by a voltage source, used to set the MZM bias angle. By adjusting the MZM RF drive voltage and bias angle, the optical modulation index (OMI) was set to $\sim 90\%$. The modulated light out of the MZM is then amplified via a high-power erbium-doped fiber amplifier (EDFA), capable of 5W average output power. A variable attenuator is then used to adjust the input optical power to photodetector under test. DC bias to the PD is provided through an external bias tee. The RF signal can then be coupled to an electrical spectrum analyzer to measure output RF power, or sent back to the LCA to determine the 3-dB high-frequency cutoff point.

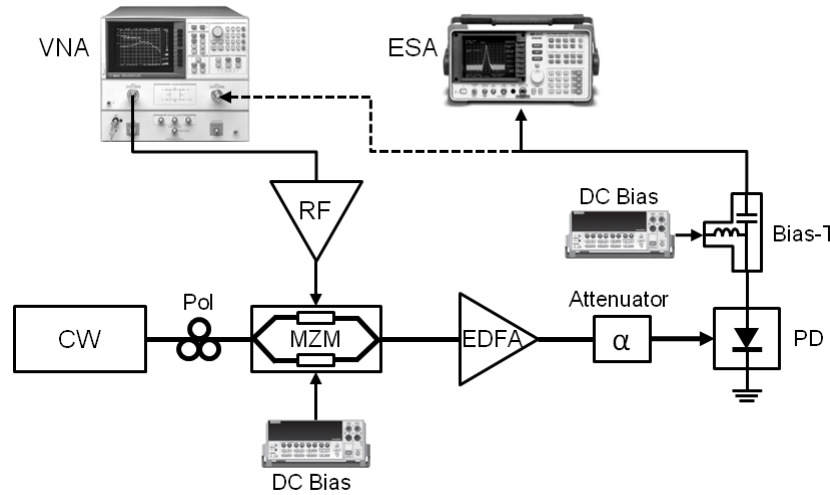


Figure 3. Schematic of test setup, used to measure 3-dB RF bandwidth and saturation output RF power.

Using the test setup, the RF output power was measured at an RF frequency of 10 GHz, held at 25°C, and with bias voltages at -6, -8, and -10V. As shown in Figure 4, the maximum, unsaturated RF output power for a 28 μm device was 20.1 dBm at bias voltage of -10V with 90 mA photocurrent, while a 34 μm device had a maximum RF output power of 21.3 dBm at bias voltage of -10V with 106 mA photocurrent. Typical responsivity ranged between 0.3 and 0.7 A/W, depending on the both fiber position and active region diameter. For high power measurements, the responsivity was

reduced by 3 dB from the maximum measured value. The ideal RF power line at 50 Ω for a modulated photocurrent (100 % modulation depth) is drawn for reference, as these devices did not utilize an impedance matching network. Due to device thermal failures at photocurrents well beyond 100 mA, the measurements in Figure 4 were limited to 100 mA.

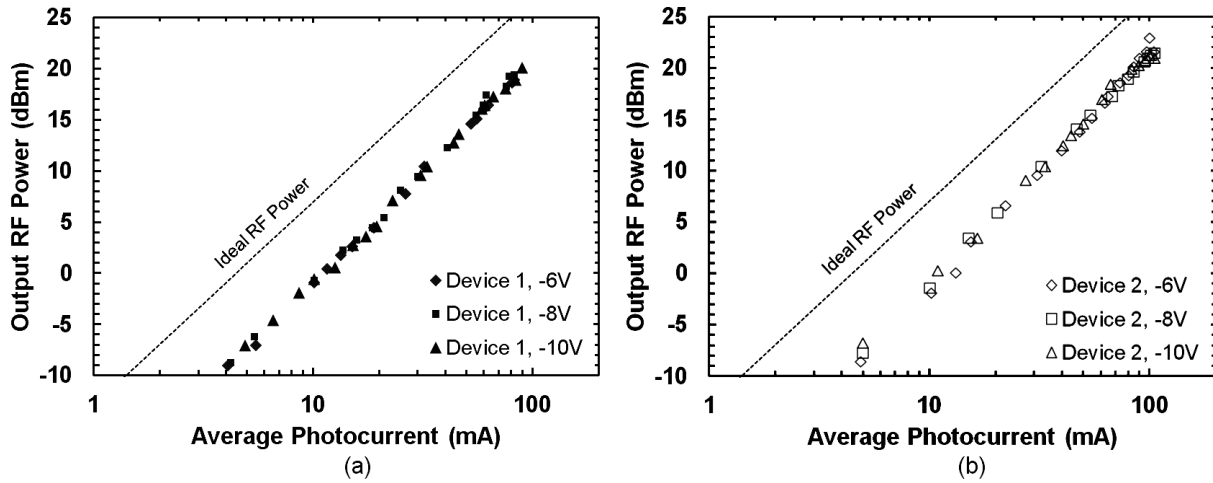


Figure 4. Measured output RF power vs. average photocurrent for two photodetectors at $f_0 = 10$ GHz, with increasing reverse bias voltage, for (a) 28 μm and (b) 34 μm diameter device. Both photodetectors demonstrate >20 dBm output power.

The same test setup in Figure 3 could also be configured to measure the optical-to-electrical (O-E) frequency response of the photodetector, to determine the 3-dB cutoff frequency. Two MUTC photodiode chip-on-submount devices were assembled into a 1.3 cm^3 low-volume package, designed at Freedom Photonics. The package includes a GPPO style coaxial RF connector, rated for 40 GHz bandwidth operation, as well as a 3-pin connector to provide DC bias. Light is coupled into the package via a SMF-28 fiber. The package also contains an integrated bias-tee network, such that external bias-tee is not required for operation.



Figure 5. Photograph of Freedom Photonics' packaged MUTC photodetector, with the lowest package volume (1.3 cm^3) and an integrated bias-tee.

With 28 μm devices assembled into a package as shown in Figure 5, the 3-dB RF bandwidth was measured, utilizing a similar test setup configuration as shown in Figure 3. As shown from measured data and fit to the data in Figure 6, the RF bandwidth was > 20 GHz. These packaged devices included an integrated bias-tee network, which also included a 50 Ω matching resistor. Due to the placement of the matching resistor, relative to the photodetector device, a ± 1 dB ripple is evident in the data as a standing wave due to an impedance mismatch. By placing the matching resistor closer to the photodiode, the ripple can be reduced. From the measured results, Freedom Photonics' packaged single MUTC photodetectors can achieve high-output RF power, > 20 dBm, and high frequency operation, > 20 GHz.

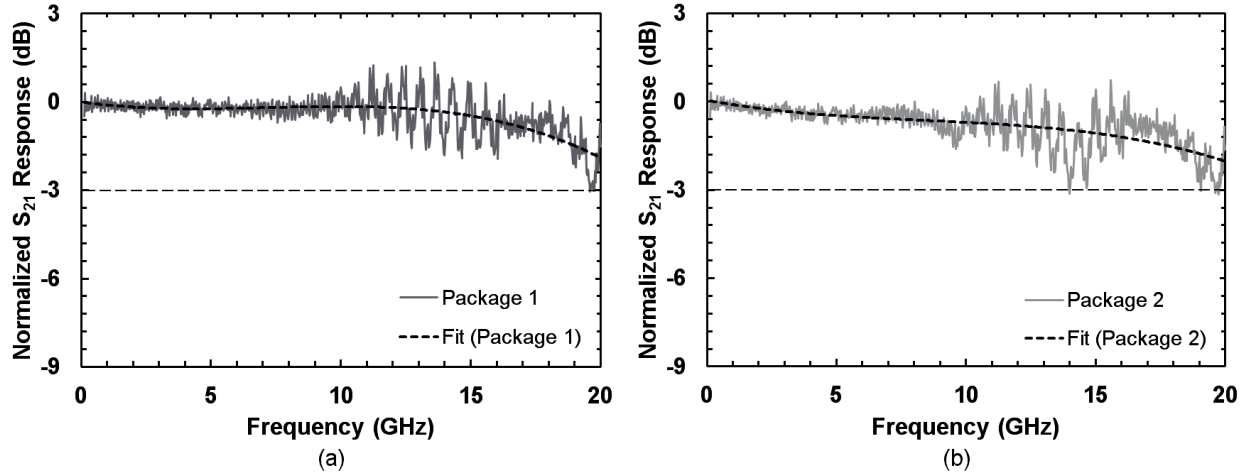


Figure 6. Normalized O-E S_{21} response of two $\text{\O}28 \mu\text{m}$ packaged single photodetectors, both exhibiting $> 20 \text{ GHz}$ 3-dB bandwidth. Measurement and fit to the data are depicted. The $\pm 1 \text{ dB}$ ripple is attributed to impedance mismatch between a 50Ω matching resistor and the photodetector.

3.2 Balanced Photodetectors

Freedom Photonics is also actively working on producing packaged balanced photodetectors. Balanced photodetectors have the added advantage of 4X output power over a single photodetector, and the ability to cancel out common mode noise, such as laser RIN. The same photodetector package developed by Freedom Photonics, is compatible with balanced photodetector chips, also providing individual photodiode bias control via an integrated bias-tee.

The University of Virginia (UVA) has previously demonstrated high-power, wideband balanced photodetectors, utilizing the same epitaxial stackup described earlier¹⁴. As shown in Figure 7, these balanced photodetectors have differential-mode bandwidths of 15 GHz at 60 mA photocurrent and 20 GHz at 40 mA, at a bias voltage of -5V, for 28 μm and 20 μm diameter active regions, respectively. In addition to high bandwidth operation at moderately high photocurrent levels, the balanced photodetectors also exhibit 25 dB common-mode rejection-ratio (CMRR). It is also evident from the data, that the individual photodiodes forming the balanced pair are very well matched in the frequency response, up to the 3-dB cutoff point.

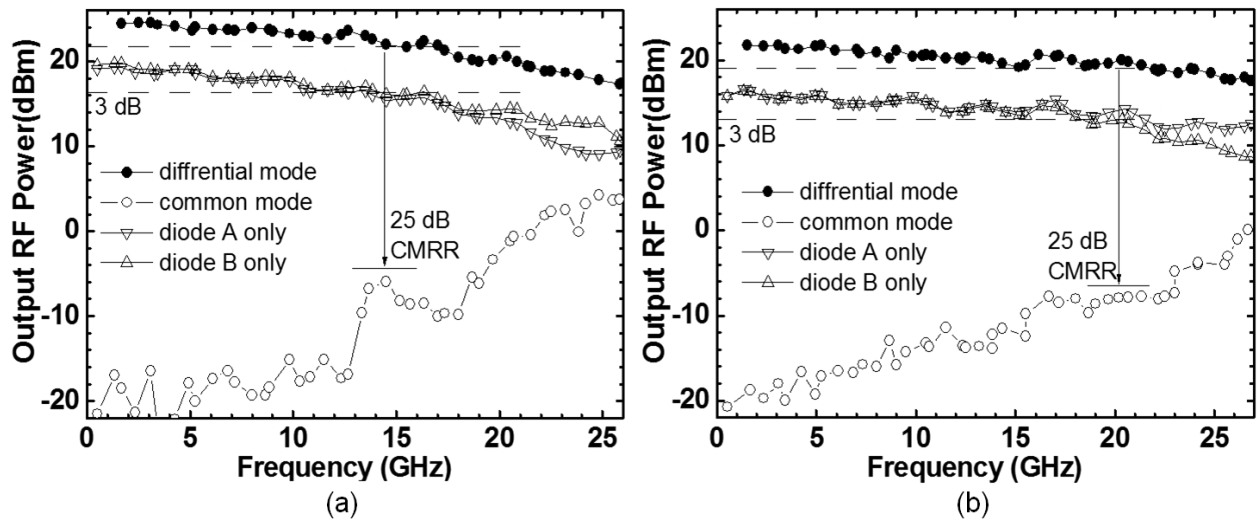


Figure 7. Balanced photodetector output power response and CMRR over frequency, for (a) 28 μm and (b) 20 μm device. Performance for each diode is also shown, exhibiting 15 GHz and 20 GHz bandwidths with 25 dB CMRR.

The maximum output RF power of the balanced photodetector pairs were also characterized, with increasing photocurrent, as shown in Figure 8. At a reverse bias voltage of 9V, the 28 μm device exhibited an output power of 27.4 dBm at 15 GHz, with 230 mA photocurrent. The 20 μm device exhibited an output power of 24.1 dBm at reverse bias voltage of 8V at 20 GHz, with a photocurrent of 139 mA.

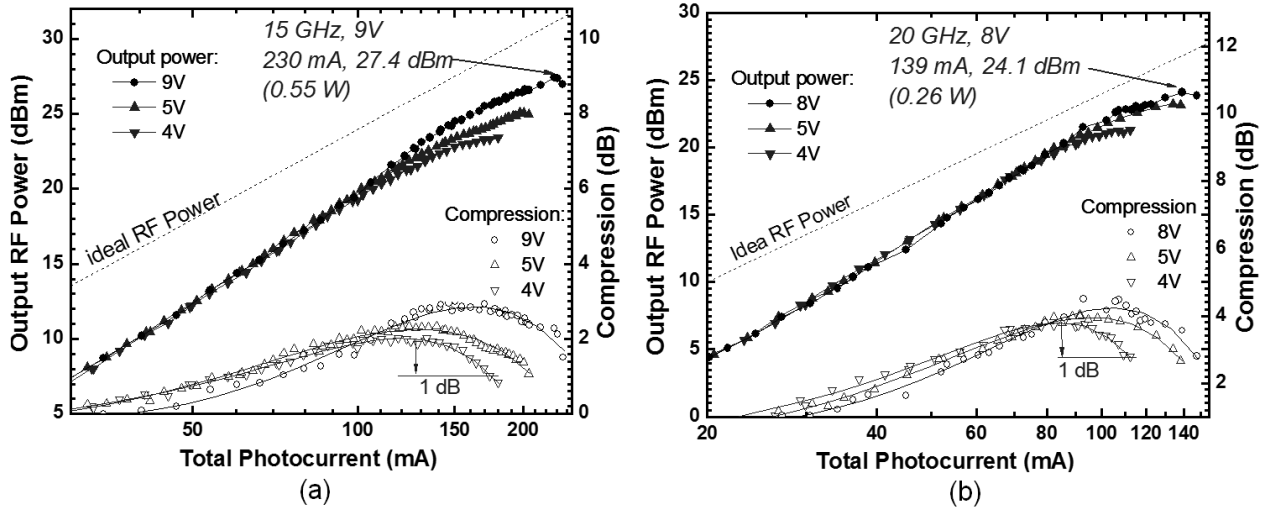


Figure 8. Output RF power and compression with increasing total photocurrent, for (a) 28 μm at 15 GHz and (b) 20 μm device at 20 GHz, for varying reverse bias voltage.

3.3 100 GHz Photodetectors

Recently, the team at UVA demonstrated high-speed MUTC PDs that achieved 9.6 dBm RF output power at 100 GHz corresponding to a saturation current of 50 mA⁹. To reduce the electron transient time the thicknesses of the drift and absorber layers in these photodiodes were decreased to 300 nm and 180 nm, respectively. PDs with diameters as small as 5 μm^2 were fabricated to reduce the junction capacitance. The flip-chip bond pads on the submount were designed to provide inductive peaking in order to further increase the bandwidth. The measured frequency responses of a 5 μm -diameter MUTC photodiode at 5 mA, 10 mA, and 15 mA average photocurrent and a reverse bias of 3.5 V are shown in Figure 9.

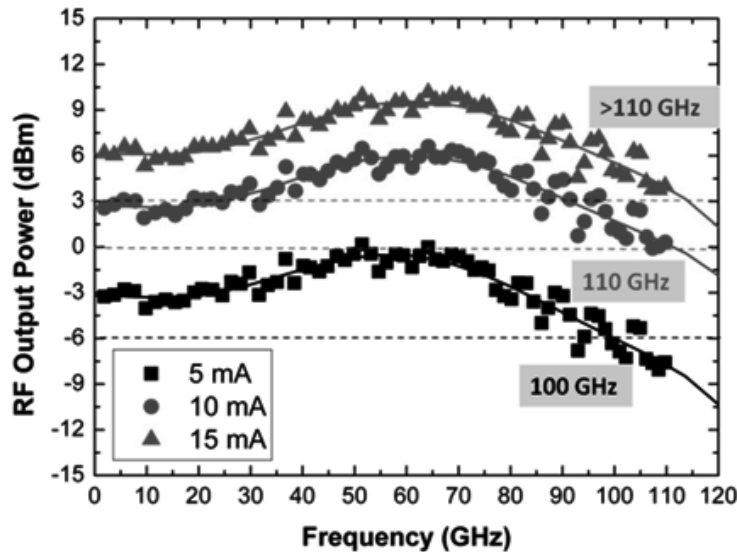


Figure 9. Measured (symbols) and fitted (lines) frequency response of a MUTC PD with 5- μm diameter at different photocurrents.

4. CONCLUSIONS

Freedom Photonics has developed packaged modified uni-traveling carrier (MUTC) photodetectors for high-power operation and applications. Both single and balanced photodetector pairs are mounted on a ceramic carrier, and packaged in a compact module optimized for high power operation. Representative results have been shown, including greater than 100mA photocurrent, >100mW generated RF power and >20GHz bandwidth. In this paper, we evaluated the saturation and bandwidth of these single ended and balanced photodetectors for detector diameters in the 16 μ m to 34 μ m range. Further new development towards the realization of >100GHz packaged photodetector modules with optimized high power performance was described. Finally, incorporation of these photodetector structures in novel photonic integrated circuits (PICs) for high optical power application areas was outlined.

REFERENCES

- [1] Seeds, Alwyn J., and Keith J. Williams. "Microwave photonics." *Journal of Lightwave Technology* 24.12, 4628-4641 (2006).
- [2] Capmany, José, et al. "Microwave photonic signal processing." *Journal of Lightwave Technology* 31.4, 571-586 (2013).
- [3] Cox III, Charles H., et al. "Limits on the performance of RF-over-fiber links and their impact on device design." *IEEE Transactions on Microwave Theory and Techniques* 54.2, 906-920 (2006).
- [4] Williams, Keith J., and Ronald D. Esman. "Design considerations for high-current photodetectors." *Journal of Lightwave Technology* 17.8, 1443-1454 (1999).
- [5] Ishibashi, T., et al. "Uni-traveling-carrier photodiodes." *Tech. Dig. Ultrafast Electronics and Optoelectronics* 13, 83-87 (1997).
- [6] Nagatsuma, Tadao, Hiroshi Ito, and Tadao Ishibashi. "High-power RF photodiodes and their applications." *Laser & Photonics Reviews* 3.1-2, 123-137 (2009).
- [7] Li, Zhi, et al. "High-saturation-current modified uni-traveling-carrier photodiode with cliff layer." *Journal of Quantum Electronics* 46.5, 626-632 (2010).
- [8] Xie, Xiaojun, et al. "Improved power conversion efficiency in high-performance photodiodes by flip-chip bonding on diamond." *Optica* 1.6, 429-435 (2014).
- [9] Q. Li, K. Li, X. Xie, Y. Fu, Z. Yang, Y. Shen, Y. Wang, A. Beling and J. C. Campbell, "High-Power Flip-Chip Bonded Photodiode with 110 GHz bandwidth," *International Conference on Photonics (ICP)*, 1-2 (2015).
- [10] Johansson, L.A, et al. "Component Development for RF Photonic Systems," *Avionics, Fiber-Optics and Photonics Conference (AVFOP)*, 38-39 (2015).
- [11] Rouvalis, Efthymios, et al. "High-power and high-linearity photodetector modules for microwave photonic applications." *Journal of Lightwave Technology* 32.20, 3810-3816 (2014).
- [12] Xie, Xiaojun, et al. "Photonic Generation of High-Power Pulsed Microwave Signals." *Journal of Lightwave Technology* 33.18, 3808-3814 (2015).
- [13] Chi, Hao, Fei Zeng, and Jianping Yao. "Photonic generation of microwave signals based on pulse shaping." *Photonics Technology Letters* 19.9, 668-670 (2007).
- [14] Zhou, Qiugui, et al. "Balanced InP/InGaAs photodiodes with 1.5-W output power." *Photonics Journal* 5.3, 6800307 (2013).

Paper presented at SPIE Photonics West 2016, San Francisco, CA, February 18th, 2016

Copyright 2016 Society of Photo-Optical Instrumentation Engineers. One print or electronic copy may be made for personal use only. Systematic reproduction and distribution, duplication of any material in this paper for a fee or for commercial purposes, or modification of the content of the paper are prohibited.